INORGANIC CHEMISTRY FRONTIERS

RESEARCH ARTICLE

View Article Online
View Journal

Cite this: DOI: 10.1039/d5qi02141c

Stepwise synthesis of symmetric and asymmetric Anderson-polyoxometalates for light-driven hydrogen evolution

Patrick Endres ,†‡[a] Garima Sachdeva,†[b] Andreas Winter, [a,c] Dolores Díaz, [a,d] Helmar Görls,[d] Nicole Fritz,[a] Christof Neumann, [e] Andrey Turchanin, [c,e] Carsten Streb [b] and Ulrich S. Schubert *[a,c,f,g]

Received 23rd October 2025,
Accepted 7th December 2025

DOI: 10.1039/d5qi02141c

rsc.li/frontiers-inorganic

A new strategy to assemble multifunctional Anderson-type polyoxometalate platforms for the light-driven hydrogen evolution reaction (HER) is presented. The stepwise coordination of precursor metal complexes enables binding of an Ir photosensitizer or a Pt HER catalyst to the bipyridine coordination site. Light-driven HER reactivity for the Pt-equipped species in homogeneous solution is reported together with initial stability analyses.

Functionalized polyoxometalates (POMs), in which organic moieties are grafted to metal–oxide clusters, have attracted widespread interest due to the ability to combine various functions (*e.g.*, light absorption, redox activity, *etc.*) into one molecular array.[1–3] Covalently organo-functionalized POMs have been used in various fields of research, including the light-driven HER, photo-electrochemistry, biomedicine, redox-active nanomaterials, (electro)catalysis, and energy storage.[4–6] Regarding the use in the context of the photochemical HER, various strategies have already been successfully demonstrated. In an intermolecular scenario, *i.e.*, the photosensitizer (PS), typically a light-absorbing transition-metal complex or an organic dye is combined with a redox-active POM. Due to strong non-covalent (*e.g.*, electrostatic) interactions between the two components, electron transfer and H_2 evolution are facilitated.[7] However, often, this approach is complex, as interactions between PS and POM can lead to undesired side reactions including ion pairing and precipitation. The alternative, *i.e.*, an intramolecular scenario, can be achieved by covalently linking metal complexes[8–10] or organic dyes[11–14] as PS to suitable organo-functionalized POMs. This has been explored using either post-synthetic modification of pre-synthesized organo-POMs[8,15–17] or by direct functionalization of an appropriate POM precursor with a suitable PS.[10] The resulting covalently linked PS-POM dyads feature H_2 evolution and have even been employed for solar-energy storage and on-demand hydrogen release.[10]

In order to increase the structural complexity of organo-functionalized POMs, the toolbox of available post-functionalization methods has been significantly extended in recent years.[2] However, the asymmetric functionalization, in particular of POMs from the Anderson-Evans family, remains challenging, but offers unique abilities to introduce two different functionalities (*e.g.*, photosensitizer and catalyst) on one POM platform.[18–22] The one-pot synthesis of asymmetric POMs using two different organic ligands is intricate due to the tedious removal of the simultaneously formed symmetric POMs.[20] Whereas, the stoichiometry-controlled one-sided modification of H_2N-[$MnMo_6O_{24}$]-NH_2, which is recognized as the "universal" precursor in this field, is often less demanding.[18] In order to establish a new route towards asymmetrically functionalized POMs, we relied on the bpy-[$MnMo_6O_{24}$]-bpy POM (**1**), which was previously used to assemble the symmetric bis-complexes **2** by coordinating $[Ir(ppy)_2]^+$ or $[Rh(ppy)_2]^+$ fragments to both of the POM's binding sites (bpy: 2,2′-bipyridine; ppy: 2-phenyl-pyridinato; Fig. 1).[16] The Ir(III)-containing derivative (**2a**) was further used as a photosensitizer-catalyst (PS-Cat) dyad for the light-driven HER.[17,23] Here, we expand this

[a]*Laboratory for Organic and Macromolecular Chemistry (IOMC), Friedrich Schiller University Jena, Humboldtstr. 10, 07743 Jena, Germany.*
E-mail: ulrich.schubert@uni-jena.de
[b]*Department of Chemistry, Johannes Gutenberg University Mainz, Duesbergweg 10-14, 55128 Mainz, Germany*
[c]*Center for Energy and Environmental Chemistry Jena (CEEC Jena), Friedrich Schiller University Jena, Philosophenweg 7a, 9774 Jena, Germany*
[d]*Institute for Inorganic and Analytical Chemistry (IAAC), Friedrich Schiller University Jena, Humboldtstr. 8, 07743 Jena, Germany*
[e]*Institute of Physical Chemistry (IPC), Friedrich Schiller University Jena, Lessingstr. 10, 07743 Jena, Germany*
[f]*Helmholtz Institute for Polymers in Energy Applications Jena (HIPOLE Jena), Lessingstr. 12-14, 07743 Jena, Germany*
[g]*Helmholtz-Zentrum Berlin für Materialien und Energie (HZB), Hahn-Meitner-Platz 1, 14109 Berlin, Germany*
†These authors contributed equally.
‡Present address: Evety GmbH c/o OGE, Bamlerstr. 1b, 45141 Essen, Germany.

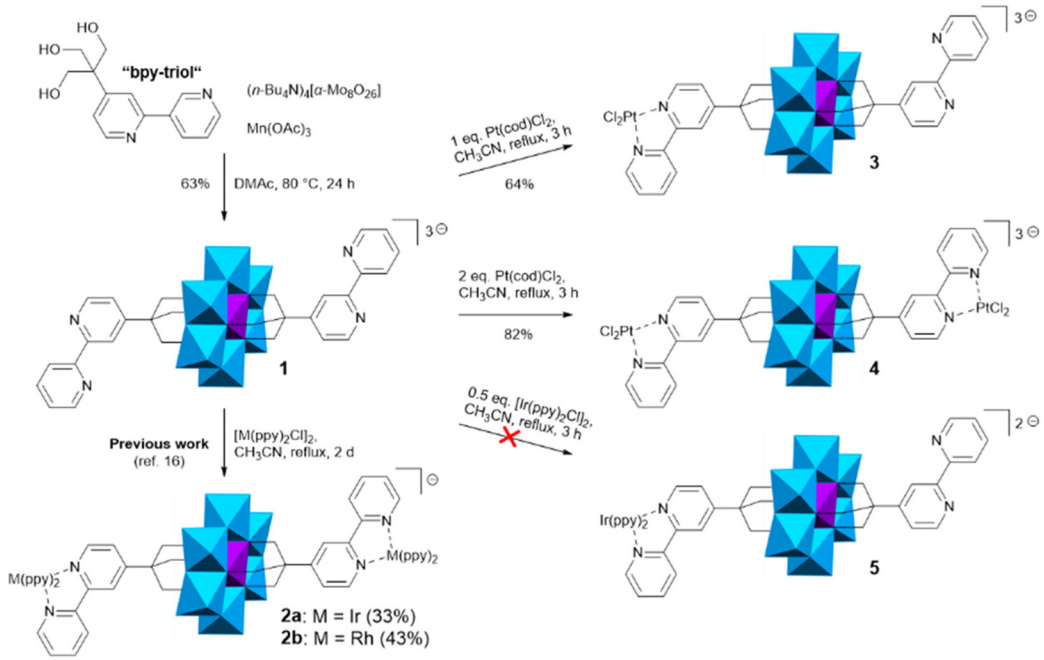

Fig. 1 Schematic representation of the synthesis of the symmetric and asymmetric complexes of bpy-[$MnMo_6O_{24}$]-bpy (**1**) with $PtCl_2$ fragments. The respective tetra(*n*-butyl)ammonium (TBA) counterions are omitted for clarity. Colour scheme for the POM moiety: Mo: blue, Mn: purple.

approach to establish a more generalized access route to symmetric and asymmetric Anderson anions, functionalized with photoactive or catalytically active metal complex fragments. The [Pt(cod)Cl_2] precursor was used to prepare the mono- and bis-complexes of **1** by a straightforward stoichiometry-controlled complexation strategy (cod: cycloocta-1,5-diene; Fig. 1). The products **3** and **4** were obtained in 82% and 64% yield, respectively, after precipitation or crystallization from the reaction mixture. The product formation was facilitated by the ease of complexation under mild conditions, that were not given when dealing with the [Ir(ppy)$_2$Cl]$_2$ precursor. The targeted synthesis of **5** remained unsuccessful and provided mixtures of products which could not be separated. Research to overcome this shortcoming is still ongoing. Compounds **3** and **4** were thoroughly characterized by NMR spectroscopy (^{1}H-, ^{195}Pt-, ^{1}H-diffusion-ordered spectroscopy (^{1}H-DOSY)), matrix-assisted laser desorption/ionization time-of flight (MALDI-TOF) mass spectrometry as well as high-resolution X-ray photoelectron spectroscopy (XPS). The ^{1}H NMR spectra featured the signal of the OCH_2 moieties at *ca.* 64 ppm (see SI). The remarkable downfield shift of the signal of the alkoxy linkage is due to its proximity to the paramagnetic Mn(III) centre, which is in a triplet high-spin state.[24] Moreover, the signals of the bpy ligand of the [Pt(bpy)Cl_2] moiety were unambiguously identified (see Fig. 2).[25,26] However, considerable signal broadening prevented the precise assignment and accurate integration. Nonetheless, due to the symmetric nature of **4**, the aromatic region revealed less signals as in the case of asymmetric **3** (this behaviour resembles that of **2a**/**b**, which were reported beforehand).[16] The ^{1}H NMR spectrum of **3**

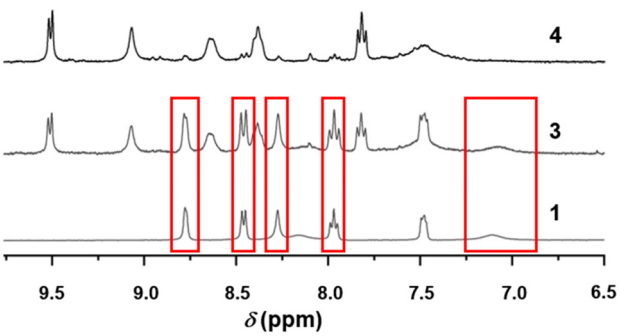

Fig. 2 ^{1}H NMR spectra of **1**, **3** and **4** (300 MHz, d_6-DMSO, 298 K). For clarity, only the aromatic region is shown here.

showed signals of the coordinated and non-coordinated bpy ligands, indicative of the selective single-site complexation of **1**. Whereas, compounds **3** and **4** could not be distinguished by ^{195}Pt NMR spectroscopy: In either case, a signal at *ca.* −2325 ppm was observed, which is in the typical range for a [Pt(bpy)Cl_2] complex.[27]

^{1}H-DOSY measurements were also carried out to confirm the structure and homogeneity of compounds **1**, as well as **3** and **4**. In all cases, the diffusion of the respective polyoxoanion – independent from the TBA (nBu$_4$N$^+$) cations – was observed (an overlay of the DOSY spectra is shown Fig. 3, the full spectra are displayed in the SI). The SEGWE model was applied to correlate the measured diffusion coefficients (D) to the calculated ones.[29,30] Albeit not developed for the analysis of complex, metal-containing molecules, such as the rigid hybrid POMs, a

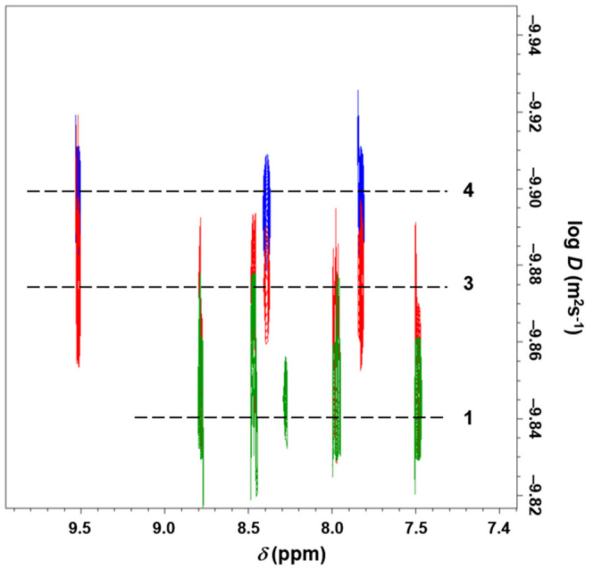

Fig. 3 Overlay of the ^{1}H-DOSY spectra of **1** (green), **3** (red) and **4** (blue) showing the diffusion behaviour of the respective polyoxoanions (500 MHz, d_6-DMSO, 298 K). For clarity, only the aromatic region is shown here, full spectra are included in the SI.

remarkably good agreement of the experimental and theoretical D values was obtained for **1**, **3** and **4** (*i.e.*, deviation of ≤4%, Table 1). Thus, ^{1}H-DOSY represents a powerful, yet rarely used method to analyse (hybrid) POMs in solution.

MALDI-TOF MS was applied to confirm the identity of **3** and **4**. However, careful optimization of the measurement conditions was required. In the case of compound **3**, the spectra were recorded in the positive reflector mode using KCl as the additive. Whereas the most meaningful spectra of **4** were obtained in the negative mode. The MALDI-TOF mass spectra of **3** and **4**, which were measured with *trans*-2-[3-(4-*tert*-butylphenyl)-2-methyl-2-propenyliden]malononitrile (DCTB), as the matrix, are displayed in the SI. In both cases, the intact polyoxoanions with accompanying TBA cations were observed. In contrast to **3**, hybrid POM **4** featured a more complex fragmentation pattern.

Furthermore, the elemental composition of compounds **3** and **4** was determined by high-resolution XPS measurements. The overview spectra, as shown in the SI, revealed the expected elements of the hybrid POMs. The relevant elemental ratios, which were derived from these spectra, were in very good agreement with the calculated ones, thus confirming the compound purity. For example, the observed Pt-to-Mn atomic ratios were 1 : 0.9 (±0.1) (for **3**) and 1 : 2.1 (±0.2) (for **4**). These ratios corroborate the success of the single-side and two-fold complexation, respectively.

In the case of compound **4**, single-crystals suitable for single-crystal X-ray diffraction (XRD) analysis were obtained by the slow diffusion of diethyl ether into a concentrated solution of **4** in CH_3CN. The XRD data revealed a strictly linear arrangement of the molecule, in which the two [Pt(bpy)Cl_2] arms were perfectly coplanar (∠Pt–Mn–Pt = 180°; Fig. 4). The intramolecular centre-to-centre distance of two Pt(II) complexes, which were oriented in a *transoid* fashion, was 18.62 Å. The bond lengths and angles of the [$MnMo_6O_{24}$] cluster were in very good agreement with the values reported elsewhere for related hybrid POMs.[16,24,31,32] Thus, the typical quintet high-spin state (S = 2) of the central Mn(II) ion is expected.[24] In particular, very little deviation from the parent structure **1** was observed in terms of bond lengths and angles.[16] The [Pt(bpy)Cl_2] fragments were slightly asymmetric; The Pt–N bonds towards the POM were elongated by a factor of *ca.* 1.1 when compared to those to the more remote N-atoms (*i.e.*, 2.0268 Å *vs.* 2.0014 Å). This suggests that the coordination *via* the pyridine rings in proximity to the cluster is slightly weaker, due to the electron-withdrawing nature of the polyoxoanion.

The crystal lattice of **4** was comprised of 1D chains, in which the individual Pt-[$MnMo_6O_{24}$]-Pt polyanions interacted *via* metallophilic interactions of their [Pt(bpy)Cl_2] complexes; thereby the adjacent Pt(II) centres were in proximity of 3.60 Å. These chains formed 2D layers, in which the chains were sep-

Table 1 Results of the ^{1}H-DOSY measurements[a]

		D (10^{-10} m^2 s^{-1})	
	M_w[b] (g mol^{-1})	Measured	Calculated[c]
1	1433.150	1.33	1.31
3	1699.142	1.27	1.25
4	1965.126	1.22	1.18

[a] Further details on the DOSY results can be found in the SI. [b] Molar mass of the polyoxoanion excluding the three TBA cations. [c] The D values were estimated using Morris' SEGWE D/MW calculator.[28]

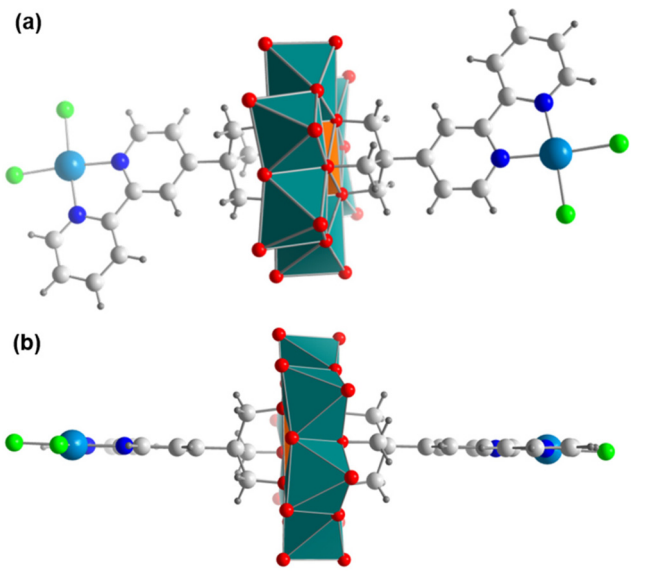

Fig. 4 (a and b) Two different views of the solid-state structure of **4** (TBA cations and solvent molecules are omitted for clarity). Colour scheme: Mo: teal, Mn: orange, Pt: light blue, Cl: green, N: dark blue, C: light grey, H: dark grey.

arated by 17.77 Å (resembling the closest distance between two Mn(III) centres of different chains). The 3D lattice represented a highly regular AB-type layered structure, in which the chains within the B layers[24] were rotated by *ca.* 90° with respect to those of the A layer. This 3D arrangement gave rise to a highly porous structure whose channels and voids contributed *ca.* 40% to the overall volume of the unit cell.

The visible-light-driven HER activity of **3** and **4** was studied using $[Ru(bpy)_3(PF_6)_2]$ as a photosensitizer (**PS**), because of its well-known ability to transfer electrons to POMs.[10,33,34] In brief, the standard catalytic studies involved water-free, de-aerated DMF solutions containing the corresponding catalyst (12.5 μM), **PS** (125 μM), triethylamine (0.9 M) as a sacrificial electron donor (SED), and water (0.7 M) as a proton source in a microwave vial. Note that DMF was chosen as a solvent due to the chemical compatibility and solubility of all relevant components. The experimental conditions were adapted from previous work.[35] The reaction solution was irradiated with a monochromatic LED source (λ_{max} = 465 nm, P ~13 mW) at ambient temperature conditions, and hydrogen evolution was measured by head-space gas chromatography. The experiments were performed in duplicate and averaged turnover numbers (TONs) are reported. Two in-house synthesized POM based catalysts, $(TBA)_3[MnMo_6O_{18}\{(OCH_2)_3C(C_6H_5)\}_2]$ (**6**)[16] and $(TBA)_3[MnMo_6O_{18}\{(OCH_2)_3CH\}_2]$ (**7**)[24] were used as references under otherwise identical conditions.

As shown in Fig. 5, significant differences in the reactivity were noticed after 7 h. Catalyst **4** exhibited turnover numbers (TONs) of *ca.* 451 (TOF *ca.* 1.1 min^{-1}), whereas **3** revealed TONs of *ca.* 345 (TOF *ca.* 0.8 min^{-1}), after seven hours of continuous irradiation. This initial data shows that the HER activity of Anderson HER-catalysts can be controlled by variation of the number of Pt-HER sites present in the catalyst. However, the data also shows that the underlying mechanism requires further analyses, as HER evolution only increases by 30%, not by 100%, as could be theoretically expected. This modest increase in TON is currently under study by time-resolved photophysical methods and computational analysis; however, one plausible explanation is the formation of supramolecular photosensitizer-catalyst aggregates which could lead to different rates of intermolecular electron transfer.

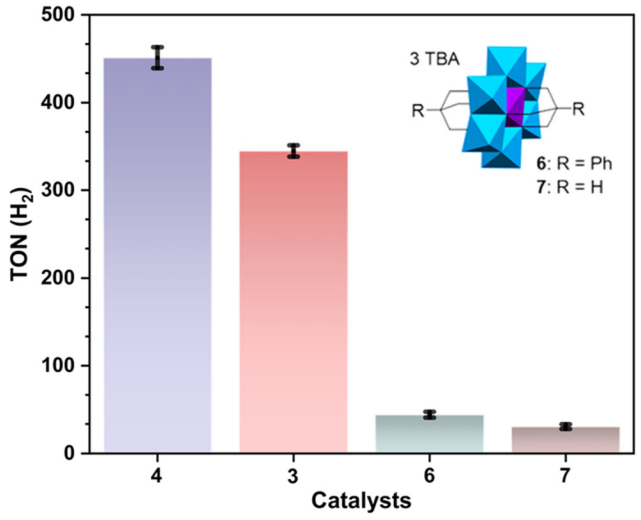

Fig. 5 Comparison of the active compounds **3** and **4**, as well as reference compounds **6** and **7** for light driven HER catalysis. Conditions: Catalyst (12.5 μM), **PS** (125 μM), TEA (0.9 M), H_2O (0.7 M), in water-free, de-oxygenated DMF, λ_{max} = 465 nm, $t_{irrad.}$ = 7 h.

In contrast, when the noble metal-free POM-based reference catalysts **6** and **7** were investigated under identical experimental conditions, only very low TONs were observed (**6**: TON = 44; **7**: TON = 30). This is in line with previous observations which suggest that the Pt-centres represent the actual HER active sites, while the pure POM exhibits only limited HER activity.[23,35–37] The observed TONs for **4** are comparable with a previous study on a di-Pt-functionalized Anderson anion, where a labile imine bond was used to link Anderson-POM to the bpy ligands.[35] For this system, TONs of *ca.* 460 were observed after 7 h irradiation when using $[Ir(ppy)_3]^+$ as a photosensitizer. Note that this system could only be operated in water-free conditions due to the hydrolytic lability of the imine bond. In contrast, the present system reaches nearly identical TONs when operated in the presence of water, demonstrating the superior stability of the purely C–C linked organo-functionalization. Detailed mechanistic and photophysical studies are planned to assess solution interactions between PS and POM, and to assess charge-transfer dynamics, supramolecular interactions, and possible back-electron transfer during catalysis.

In sum, this study reports the symmetric and asymmetric functionalization of an Anderson polyoxomolybdate with one or two Pt(I)-complex reaction sites, enabling the light-driven hydrogen evolution reaction when combined with a Ru(II)-based metal-complex photosensitizer. The study demonstrates that the number of Pt sites controls HER activity and paves the way for the design of molecular dyads where in principle, a metal complex PS and a metal complex catalyst could be combined in one molecule. Also, replacement of the noble metal complexes with noble metal-free analogues can be envisaged for enhanced technological relevance.

Author contributions

P. E. – investigation and visualization; G. S. – data curation, investigation, visualization, and writing – original draft; A. W. – conceptualization, supervision, validation, visualization, writing – original draft; D. D. – data curation, formal analysis, investigation, validation, visualization, writing – original draft; H. G. – data curation, formal analysis, investigation, validation, visualization, writing – original draft; N. F. – data curation, investigation; C. N. – data curation, formal analysis, investigation, validation, visualization, writing – original draft; A. T. – funding acquisition, project administration, resources, supervision, writing – review & editing; C. S. – conceptualiz-

ation, funding acquisition, project administration, resources, supervision, visualization, writing – review & editing; U. S. S. – funding acquisition, project administration, resources, supervision, writing – review & editing.

Conflicts of interest

There are no conflicts to declare.

Data availability

The experimental data supporting this article have been included as part of the supplementary information (SI). Supplementary information is available. See DOI: **https://doi.org/10.1039/d5qi02141c**.

CCDC 2484790 (**4**) contains the supplementary crystallographic data for this paper.[38]

Acknowledgements

The authors gratefully acknowledge financial support by the Deutsche Forschungsgemeinschaft (DFG) within the Priority Program "Light-controlled reactivity of metal complexes" (SPP-2102, LCRMC, project number 493768838) and the Collaborative Research Centre TRR 234 "CataLight" (project number: 364549901; projects A4, A5, B2, B3, B7, B9 and Z2). Moreover, the Thüringer Aufbaubank (TAB) supported the acquisition of the rapifleX MALDI TOF/TOF spectrometer (grant number 2016/IZN/0009). Likewise, the authors thank the DFG for their support in acquiring the XPS and the 500 MHz NMR spectrometer (infrastructure grants INST 275/25 7-1 FUGG and INST 275/442-1 FUGG, respectively).

References

1 A. Proust, B. Matt, R. Villanneau, G. Guillemot, P. Gouzerh and G. Izzet, Functionalization and post-functionalization: A step towards polyoxometalate-based materials, *Chem. Soc. Rev.*, 2012, **41**, 7605–7622, DOI: **10.1039/C2CS35119F**.

2 A. V. Anyushin, A. Kondinski and T. N. Parac-Vogt, Hybrid polyoxometalates as post-functionalization platforms: From fundamentals to emerging applications, *Chem. Soc. Rev.*, 2020, **49**, 382–432, DOI: **10.1039/C8CS00854J**.

3 J. M. Cameron, G. Guillemot, T. Galambos, S. S. Amin, E. Hampson, K. Mall Haidaraly, G. N. Newton and G. Izzet, Supramolecular assemblies of organo-functionalised hybrid polyoxometalates: From functional building blocks to hierarchical nanomaterials, *Chem. Soc. Rev.*, 2022, **51**, 293–328, DOI: **10.1039/D1CS00832C**.

4 Y. Zhang, Y. Li, H. Guo, Y. Guo and R. Song, Recent advances in polyoxometalate-based materials and their derivatives for electrocatalysis and energy storage, *Mater. Chem. Front.*, 2024, **8**, 732–768, DOI: **10.1039/D3QM01000G**.

5 M. J. W. Budych, K. Staszak, A. Bajek, F. Pniewski, R. Jastrząb, M. Staszak, B. Tylkowski and K. Wieszczycka, The future of polyoxymetalates for biological and chemical apllications, *Coord. Chem. Rev.*, 2023, **493**, 215306, DOI: **10.1016/j.ccr.2023.215306**.

6 J. J. Walsh, A. M. Bond, R. J. Forster and T. E. Keyes, Hybrid polyoxometalate materials for photo(electro-) chemical applications, *Coord. Chem. Rev.*, 2016, **306**, 217–234, DOI: **10.1016/j.ccr.2015.06.016**.

7 L. Qin, C. Zhao, L.-Y. Yao, H. Dou, M. Zhang, J. Xie, T.-C. Weng, H. Lv and G.-Y. Yang, Efficient photogeneration of hydrogen boosted by long-lived dye-modified Ir(III) photosensitizers and polyoxometalate catalyst, *CCS Chem.*, 2022, **4**, 259–271, DOI: **10.31635/ccschem.021.202000741**.

8 B. Matt, J. Fize, J. Moussa, H. Amouri, A. Pereira, V. Artero, G. Izzet and A. Proust, Charge photo-accumulation and photocatalytic hydrogen evolution under visible light at an iridium(III)-photosensitized polyoxotungstate, *Energy Environ. Sci.*, 2013, **6**, 1504–1508, DOI: **10.1039/C3EE40352A**.

9 D. Schaming, C. Allain, R. Farha, M. Goldmann, S. Lobstein, A. Giraudeau, B. Hasenknopf and L. Ruhlmann, Synthesis and photocatalytic properties of mixed polyoxometalate–porphyrin copolymers obtained from Anderson-type polyoxomolybdates, *Langmuir*, 2010, **26**, 5101–5109, DOI: **10.1021/la903564d**.

10 S. Amthor, S. Knoll, M. Heiland, L. Zedler, C. Li, D. Nauroozi, W. Tobaschus, A. K. Mengele, M. Anjass, U. S. Schubert, B. Dietzek-Ivanšić, S. Rau and C. Streb, A photosensitizer–polyoxometalate dyad that enables the decoupling of light and dark reactions for delayed on-demand solar hydrogen production, *Nat. Chem.*, 2022, **14**, 321–327, DOI: **10.1038/s41557-021-00850-8**.

11 G. Toupalas, J. Karlsson, F. A. Black, A. Masip-Sánchez, X. López, Y. Ben M'Barek, S. Blanchard, A. Proust, S. Alves, P. Chabera, I. P. Clark, T. Pullerits, J. M. Poblet, E. A. Gibson and G. Izzet, Tuning photoinduced electron transfer in POM-BODIPY hybrids by controlling the environment: Experiment and theory, *Angew. Chem., Int. Ed.*, 2021, **60**, 6518–6525, DOI: **10.1002/anie.202014677**.

12 S. Cetindere, S. T. Clausing, M. Anjass, Y. Luo, S. Kupfer, B. Dietzek and C. Streb, Covalent linkage of BODIPY-photosensitizers to Anderson-type polyoxometalates using CLICK chemistry, *Chem. – Eur. J.*, 2021, **27**, 17181–17187, DOI: **10.1002/chem.202102897**.

13 F. Odobel, M. Séverac, Y. Pellegrin, E. Blart, C. Fosse, C. Cannizzo, C. R. Mayer, K. J. Elliott and A. Harriman, Coupled sensitizer–catalyst dyads: Electron-transfer reactions in a perylene–polyoxometalate conjugate, *Chem. – Eur. J.*, 2009, **15**, 3130–3138, DOI: **10.1002/chem.200801880**.

14 F. A. Black, A. Jacquart, G. Toupalas, S. Alves, A. Proust, I. P. Clark, E. A. Gibson and G. Izzet, Rapid photoinduced charge injection into covalent polyoxometalate–bodipy con-

jugates, *Chem. Sci.*, 2018, **9**, 5578–5584, DOI: 10.1039/C8SC00862K.

15 S. Schönweiz, M. Heiland, M. Anjass, T. Jacob, S. Rau and C. Streb, Experimental and theoretical investigation of the light-driven hydrogen evolution by polyoxometalate–photosensitizer dyads, *Chem. – Eur. J.*, 2017, **23**, 15370–15376, DOI: 10.1002/chem.201702116.

16 A. Winter, P. Endres, E. Schröter, M. Jäger, H. Görls, C. Neumann, A. Turchanin and U. S. Schubert, Towards covalent photosensitizer-polyoxometalate dyads-bipyridyl-functionalized polyoxometalates and their transition metal complexes, *Molecules*, 2019, **24**, 4446, DOI: 10.3390/molecules24244446.

17 Y. Luo, S. Maloul, P. Endres, S. Schönweiz, C. Ritchie, M. Wächtler, A. Winter, U. S. Schubert, C. Streb and B. Dietzek, Organic linkage controls the photophysical properties of covalent photosensitizer–polyoxometalate hydrogen evolution dyads, *Sustainable Energy Fuels*, 2020, **4**, 4688–4693, DOI: 10.1039/D0SE00582G.

18 Q. Zhuang, Z. Sun, C.-G. Lin, B. Qi and Y.-F. Song, Latest progress in asymmetrically functionalized Anderson-type polyoxometalates, *Inorg. Chem. Front.*, 2023, **10**, 1695–1711, DOI: 10.1039/D2QI02690B.

19 M. H. Rosnes, C. Musumeci, C. P. Pradeep, J. S. Mathieson, D.-L. Long, Y.-F. Song, B. Pignataro, R. Cogdell and L. Cronin, Assembly of modular asymmetric organic–inorganic polyoxometalate hybrids into anisotropic nanostructures, *J. Am. Chem. Soc.*, 2010, **132**, 15490–15492, DOI: 10.1021/ja1066338.

20 C. Yvon, A. Macdonell, S. Buchwald, A. J. Surman, N. Follet, J. Alex, D.-L. Long and L. Cronin, A collection of robust methodologies for the preparation of asymmetric hybrid Mn–Anderson polyoxometalates for multifunctional materials, *Chem. Sci.*, 2013, **4**, 3810–3817, DOI: 10.1039/C3SC51618K.

21 M.-M. Zhang, Y.-A. Yin, W.-J. Chen, C.-G. Lin, Y. Wei and Y.-F. Song, Asymmetric modification of Anderson-type polyoxometalates towards organic–inorganic homo- and hetero-cluster oligomers, *Inorg. Chem. Front.*, 2023, **10**, 1712–1720, DOI: 10.1039/D2QI02233H.

22 P. Wu, Y. Wang, B. Huang and Z. Xiao, Anderson-type polyoxometalates: From structures to functions, *Nanoscale*, 2021, **13**, 7119–7133, DOI: 10.1039/D1NR00397F.

23 Y. Luo, S. Maloul, M. Wächtler, A. Winter, U. S. Schubert, C. Streb and B. Dietzek, Is electron ping-pong limiting the catalytic hydrogen evolution activity in covalent photosensitizer–polyoxometalate dyads?, *Chem. Commun.*, 2020, **56**, 10485–10488, DOI: 10.1039/D0CC04509H.

24 A. Winter, P. Endres, N. Singh, N. E. Schlörer, H. Görls, S. Kupfer and U. S. Schubert, A missing member of the Anderson-Evans family: Synthesis and characterization of the trimethylolmethane-capped $\{MnMo_6O_{24}\}$ cluster, *Inorganics*, 2025, **13**, 254, DOI: 10.3390/inorganics13080254.

25 M. G. Pfeffer, B. Schäfer, G. Smolentsev, J. Uhlig, E. Nazarenko, J. Guthmuller, C. Kuhnt, M. Wächtler, B. Dietzek, V. Sundström and S. Rau, Palladium versus platinum: The metal in the catalytic center of a molecular photocatalyst determines the mechanism of the hydrogen production with visible light, *Angew. Chem., Int. Ed.*, 2015, **54**, 5044–5048, DOI: 10.1002/anie.201409438.

26 M. Lämmle, A. K. Mengele, G. E. Shillito, S. Kupfer and S. Rau, Stability of catalytic centres in light-driven hydrogen evolution by di- and oligonuclear photocatalysts, *Chem. – Eur. J.*, 2023, **29**, e202202722, DOI: 10.1002/chem.202202722.

27 T. Pawlak, L. Pazderski, J. Sitkowski, L. Kozerski and E. Szłyk, ^{1}H, ^{13}C, ^{195}Pt and ^{15}N NMR structural correlations in Pd(II) and Pt(II) chloride complexes with various alkyl and aryl derivatives of 2,2′-bipyridine and 1,10-phenanthroline, *Magn. Reson. Chem.*, 2011, **49**, 59–64, DOI: 10.1002/mrc.2704.

28 Estimation of Diffusion Coefficients, https://nmr.chemistry.manchester.ac.uk/?q=node/432, (accessed 2025-10-01).

29 R. Evans, G. Dal Poggetto, M. Nilsson and G. A. Morris, Improving the Interpretation of small molecule diffusion coefficients, *Anal. Chem.*, 2018, **90**, 3987–3994, DOI: 10.1021/acs.analchem.7b05032.

30 R. Evans, Z. Deng, A. K. Rogerson, A. S. McLachlan, J. J. Richards, M. Nilsson and G. A. Morris, Quantitative interpretation of diffusion-ordered NMR spectra: Can we rationalize small molecule diffusion coefficients?, *Angew. Chem., Int. Ed.*, 2013, **52**, 3199–3202, DOI: 10.1002/anie.201207403.

31 P. R. Marcoux, B. Hasenknopf, J. Vaissermann and P. Gouzerh, Developing remote metal binding sites in heteropolymolybdates, *Eur. J. Inorg. Chem.*, 2003, 2406–2412, DOI: 10.1002/ejic.200200677.

32 B. Hasenknopf, R. Delmont, P. Herson and P. Gouzerh, Anderson-type heteropolymolybdates containing tris (alkoxo) ligands: Synthesis and structural characterization, *Eur. J. Inorg. Chem.*, 2002, 1081–1087, DOI: 10.1002/1099-0682(200205)2002:5<1081::AID-EJIC1081>3.0.CO;2-W.

33 H. Lv, J. Song, H. Zhu, Y. V. Geletii, J. Bacsa, C. Zhao, T. Lian, D. G. Musaev and C. L. Hill, Visible-light-driven hydrogen evolution from water using a noble-metal-free polyoxometalate catalyst, *J. Catal.*, 2013, **307**, 48–54, DOI: 10.1016/j.jcat.2013.06.028.

34 A. Solé-Daura, Y. Benseghir, M.-H. Ha-Thi, M. Fontecave, P. Mialane, A. Dolbecq and C. Mellot-Draznieks, Origin of the boosting effect of polyoxometalates in photocatalysis: The case of CO_2 reduction by a Rh-containing metal–organic framework, *ACS Catal.*, 2022, **12**, 9244–9255, DOI: 10.1021/acscatal.2c02088.

35 S. Maloul, M. van den Borg, C. Müller, L. Zedler, A. K. Mengele, D. Gaissmaier, T. Jacob, S. Rau, B. Dietzek-Ivanšić and C. Streb, Multifunctional polyoxometalate platforms for supramolecular light-driven hydrogen evolution, *Chem. – Eur. J.*, 2021, **27**, 16846–16852, DOI: 10.1002/chem.202103817.

36 S. Schönweiz, S. A. Rommel, J. Kübel, M. Micheel, B. Dietzek, S. Rau and C. Streb, Covalent photosensitizer–polyoxometalate-catalyst dyads for visible-light-driven

hydrogen evolution, *Chem. – Eur. J.*, 2016, **22**, 12002–12005, DOI: **10.1002/chem.201602850**.

37 Y. Luo, S. Maloul, S. Schönweiz, M. Wächtler, C. Streb and B. Dietzek, Yield—not only lifetime—of the photoinduced charge-separated state in iridium complex–polyoxometalate dyads impact their hydrogen evolution reactivity, *Chem. – Eur. J.*, 2020, **26**, 8045–8052, DOI: **10.1002/chem.202000982**.

38 CCDC 2484790: Experimental Crystal Structure Determination, 2025, DOI: **10.5517/ccdc.csd.cc2pdmj8**.